Microchimica Acta
https://doi.org/10.1007/s00604-018-2686-9

ORIGINAL PAPER

Electrochemical prostate specific antigen aptasensor based on hemin functionalized graphene-conjugated palladium nanocomposites

Guojuan Zhang[1] · Zhiguang Liu[1] · Lifang Fan[1] · Yujing Guo[1]

Received: 20 September 2017 / Accepted: 17 January 2018

Abstract

An electrochemical aptasensor is described for the detection of prostate specific antigen (PSA). The aptasensor is based on the use of hemin-functionalized graphene-conjugated palladium nanoparticles (H-Gr/PdNPs) deposited on a glassy carbon electrode. The nanocomposites integrate the high electrical conductivity of graphene with the easily functionalized surface chemistry of PdNPs and their excellent catalytic property. The hemin placed on graphene acts as both a protective agent and an in-situ redox probe. The PdNPs provide numerous binding sites for the immobilization of DNA-biotin via coordinative binding between Pd and amino groups. A sensitive and specific PSA assay was attained by immobilizing the PSA aptamer via biotin-streptavidin interaction. The resulting aptasensor has a linear response that covers the PSA concentration range from 0.025 to 205 ng·mL^{-1}, with a 8 pg·mL^{-1} lower detection limit (at −0.362 V, scan rate: 0.1 mV·s^{-1}, S/N = 3). The method was applied to the quantitation of PSA in spiked serum samples, giving recoveries ranging from 95.0 to 100.3%.

Keywords Graphene · PdNPs · Hemin · Nanocomposites · Biotin-streptavidin · Aptamer · Electrochemical biosensor · Prostate specific antigen · Differential pulse voltammetry · Detection

Introduction

Prostate specific antigen (PSA), an important cancer biomarker, has been utilized for diagnosis of prostate diseases, such as prostatic cancer, prostatitis and prostatic hyperplasia [1, 2]. The common concentration of PSA in serum is 4.0-10 ng·mL^{-1} for healthy men [3–5]. Any disruptions of prostate will affect the release of PSA into the blood stream and cause the total PSA level to exceed the cut-off value ultimately. Therefore, highly sensitive and specific methods for PSA detection have great significance for early accurate diagnosis of prostate disease and protect the prostate disease from worsening sequentially [6]. To date, the methods for measuring PSA include electrochemical immunoassay [7], immune-sensors, fluorescence [8], surface plasmon resonance [9], mass spectrometry [10] and electrochemical aptasensor [11–13]. Comparatively, electrochemical aptasensors are much superior due to the advantages of low cost and simple device portability of electrochemical method together with the high affinity and specificity of aptamers and their corresponding targets [14].

In order to improve the sensitivity of the analytical method, a large number of nanomaterials have been employed due to their advantages of high surface areas, high loading of receptor molecules and unique electro-catalytic properties [15, 16]. For instance, Esmaeil presented an electrochemical aptasensor to detect PSA based on rGO-MWCNT. The sensor exhibited good selectivity towards co-existing molecules [13]. Rahi fabricated an electrochemical aptasensor with gold-nanospears which was successfully applied to detect PSA [11]. Graphene, as an excellent electrically conductive nanomaterial, has been used as the most common enhanced material for the electrochemical sensors. In particular, a series of graphene-based composites, such as graphene-metal nanoparticles and graphene-metal oxide nanocomposites have triggered extreme interest in electrochemical sensor because they displayed synergic effect of catalytic characters of both graphene and metal nanomaterials [17, 18]. PdNPs were widely used in many fields owing to their high surface areas, good biocompatibility, excellent electro-catalytic activity and high electrical conductivity.

Electronic supplementary material The online version of this article (https://doi.org/10.1007/s00604-018-2686-9) contains supplementary material, which is available to authorized users.

✉ Yujing Guo
guoyj@sxu.edu.cn

[1] Institute of Environmental Science, Shanxi University, Taiyuan 030006, China

Published online: 06 February 2018

Therefore, introducing PdNPs into the sensor will enhance the electron transfer rate and amplify electrochemical signal as well as providing binding sites for aptamers through coordinate bond between Pd and -NH_2. Additionally, the biotin-streptavidin system is constantly utilized to enhance the detection sensitivity. Streptavidin (SA) can act as an adaptor for linking any kind of biotinylated molecule to a lipid monolayer due to high-affinity between biotin and streptavidin. Furthermore, the improvement of the sensitivity is owing to four binding sites of SA for biotin binding on the SA [19–21]. Inspired by this idea, we postulate that biotin-streptavidin system is able to offer more sites to increase the primer/aptamer ratio, so as to achieve a higher sensitivity.

Another important factor for the construction of the sensitive sensor is the in-situ probes. Hemin, a well-known natural metalloporphyrin, has the peroxidase-like activity similar to the peroxidase enzyme. It also possesses predictable rigid structures, which would combine with graphene by hydrogen bonding and π interactions. Particularly, hemin can be used as electron media based on the reversible redox of Fe(III)/Fe(II). Therefore, introducing hemin in the nanocomposites not only prevents graphene from aggregation but also provides an in-situ electrochemical probe through the reversible $hemin_{ox}$/$hemin_{red}$ pair.

In the present work, a signal amplified electrochemical aptasensor was developed for PSA detection based on hemin-functionalized graphene-conjugated palladium nanoparticles (H-Gr/PdNP). The nanocomposites integrate the high electrical conductivity and large surface area of graphene, easily functionalized surface and admirable catalytic property of PdNPs together with the excellent redox properties of hemin [22]. The DNA-Biotin can attach to the H-Gr/PdNP electrode via the interaction between Pd and -NH_2. Then SA is immobilized on the DNA-biotin surface. Subsequently, PSA aptamers (PSAa) are firmly assembled on the electrode by biotin-streptavidin interaction. Therefore, the signal of hemin gradually declines due to the layer-by-layer coverage of PSAa, SA and DNA-biotin. When PSA is added, some PSAa-SA-DNA-biotin is pulled off from the H-Gr/PdNP modified electrode by the interaction of PSA and PSAa. Thus the peak current enhances. According to the changes of the peak current, an electrochemical aptasensor is established with broad linear range and good specificity. This sensing strategy offers a promising way to determine PSA in clinical diagnostics.

Materials and methods

Materials and instruments

Graphite was purchased from Alfa Aesar and hemin from Aladdin-reagent Co. (Shanghai, China, www.aladdin-e.com). Poly(dimethyl diallyl ammonium chloride) (PDDA, Mw = 400,000-500,000, 20 wt% in water) was purchased from Sigma-aldrich Co. (Louis, USA, www.sigmaaldrich.com) and K_2PdCl_4 was obtained from Beijing Chemical Reagent Factory (Beijing, China, www.crc-bj.com). Prostate specific antigen (PSA) was purchased from EMD Millipore Corp. Billerica, MA (USA, www.millipore.com). Bovine serum albumin (BSA), human serum albumin (HSA), thrombin, intravenous gamma globulin (IgG) and carcinoembryonic antigen (CEA) were obtained from Sigma-aldrich Co. (Louis, USA, www.sigmaaldrich.com). The human serum samples were provided from the local hospital. The PSA aptamer (PSAa): 5′-biotin-TTT TTA ATT AAA GCT CGC CAT CAA ATA GCT TT-3′ [23, 24], DNA-Biotin: 5′-biotin-TAT AGT CGA TCC GGA-$(CH_2)_6$-NH_2-3′ was purchased from Shanghai Sangon Biotech Co., Ltd.(Shanghai, China, www.sangon.com) and dissolved in Tris-buffer (20 mmol·L^{-1} Tri-HCl, 0.10 mol·L^{-1} NaCl, 5.0 mmol·L^{-1} $MgCl_2$, pH = 7.4). Streptavidin (SA) was purchased from BBI Life Science (www.bbi-lifesciences.com). All reagents were analytical grade, and water used throughout all experiments was purified with the Millipore system (18.2 MΩ·cm, Millipore water Ltd., USA, www.millipore.com).

UV-vis absorption spectra were recorded on a U-3010 spectrometer (Hitachi, Ltd., Tokyo, Japan, www.hitachi.com.cn). Fourier-transformation infrared (FT-IR) spectra were recorded on a Shimadzu 8400S spectrometer (Shimadzu, Kyoto, Japan, www.shimadzu.com). The morphology of the nanocomposite was recorded on a JEOL-2100 TEM (Electron Ltd., Tokyo, Japan, http://www.jeolusa.com) with an accelerating voltage of 200 kV. X-ray photoelectron spectroscopy (XPS) measurement was performed on an ESCALAB-MKII 250 photoelectron spectrometer (VG Co., New York, USA) with Al Kα X-ray radiation as the X-ray source for excitation. Electrochemical measurements were conducted on a Princeton Applied Research (PAR 4000, PMl-500) Workstation (AMETEK America, www.princeton applied research.com) with a conventional three-electrode system composed of a bare or modified glassy carbon electrode (GCE, 3.0 mm in diameter, Shanghai Chenhua Instrument Co., China; www.chinstr.com) as the working electrode, and a platinum wire and a saturated calomel electrode (SCE) as the counter electrode and the reference electrode, respectively.

Synthesis of the hemin-functionalized graphene (H-Gr) and H-Gr/PdNPs

The graphite oxide (GO) was synthesized from graphite powder according to a modified Hummers method [25]. H-Gr was prepared via π interactions between reduced graphene oxide (rGO) and hemin. Briefly, 2.5 mL of 1.0 mg·mL^{-1} GO was mixed with 2.5 mL 1.0 mg·mL^{-1} hemin, then 100 μL of ammonia solution and 10 μL of hydrazine solution were added into above. The mixture was sharply shaken for 15 min and heated at 60 °C for 3.5 h. The stable black suspension was obtained and the

supernatant with impurities were removed by centrifugation (12,000 rpm, 9576 g) to obtain H-Gr. Then, the precipitate was washed for two times with deionized water and dispersed readily in water by ultra-sonication eventually.

The H-Gr/PdNP was synthesized as follows: 50 μL of PDDA (4 wt%) was added into 2.0 mL of 0.25 mg·mL^{-1} H-Gr aqueous dispersion in a 10 mL reaction system and stirred for a few minutes. Then 200 μL of 10 mg·mL^{-1} K_2PdCl_4 was added into the vial. After several minutes, 2.0 mL of 20 mmol·L^{-1} freshly prepared $NaBH_4$ solution was slowly added to the mixing solution. After stirring for 30 min, the H-Gr/PdNP was precipitated by centrifugation and washed two times with distilled water.

Construction of the biosensor

Prior to modification, GCE was polished to a mirror-like surface with 0.03 μm and 0.05 μm alumina powder. Then, 8.0 μL of 0.5 mg·mL^{-1} H-Gr/PdNP dispersion was carefully dropped on the surface of the GCE to obtain H-Gr/PdNP/GCE. Subsequently, 8.0 μL of 5.0 μmol·L^{-1} DNA-Biotin was cast onto H-Gr/PdNP/GCE and stored at 4 °C in a refrigerator overnight. Then, the electrode was immersed in 1.0% BSA for 30 min to block the possible remaining active sites and eliminate nonspecific binding sites. Thus, the electrode of DNA-Biotin/H-Gr/PdNP/GCE was obtained. After that, 10 μL of 1.0 μg·mL^{-1} SA solution was dropped on the above electrode for 1.0 h at room temperature via streptavidin-biotin affinity. Finally, the electrode was immersed in 30 μL of 5.0 μmol·L^{-1} PSAa for additional 1.0 h at 4 °C and the electrochemical biosensor of PSAa-SA-DNA-Biotin/H-Gr/PdNP/GCE was constructed successfully.

Analysis of PSA

PSA solutions with different concentrations were added into electrolyte solution, and then incubated with the PSAa-SA-DNA-Biotin/H-Gr/PdNP/GCE for 60 min at room temperature. Differential pulse voltammetry (DPV) was conducted to express the response for the PSA by measuring the peak current changes. DPV measurements were recorded from −0.8 V to 0 V with the parameters of amplitude: 50 mV, pulse width: 0.050 s. All the electrochemical measurements were conducted with the same procedures mentioned above. And the whole experiment was performed in 0.10 mol·L^{-1} phosphate buffered saline (PBS, pH 7.4) containing 0.9% NaCl.

Results and discussion

The strategies of the biosensor for PSA detection

The process for fabricating PSAa-SA-DNA-Biotin/H-Gr/PdNP/GCE and the electrochemical sensing platform is shown in Scheme 1. H-Gr is prepared by a wet-chemical reaction under alkaline condition according to the literature [26]. Hemin, with a large planar aromatic surface, can stabilize graphene by π interactions. It also can be used as electron media through the reversible $hemin_{ox}$/$hemin_{red}$ pair. Introducing PdNPs into H-Gr can improve electron transfer and enhance the electrochemical signal [27]. They are also able to provide binding sites for DNA-Biotin immobilization, which subsequently conjugate with SA

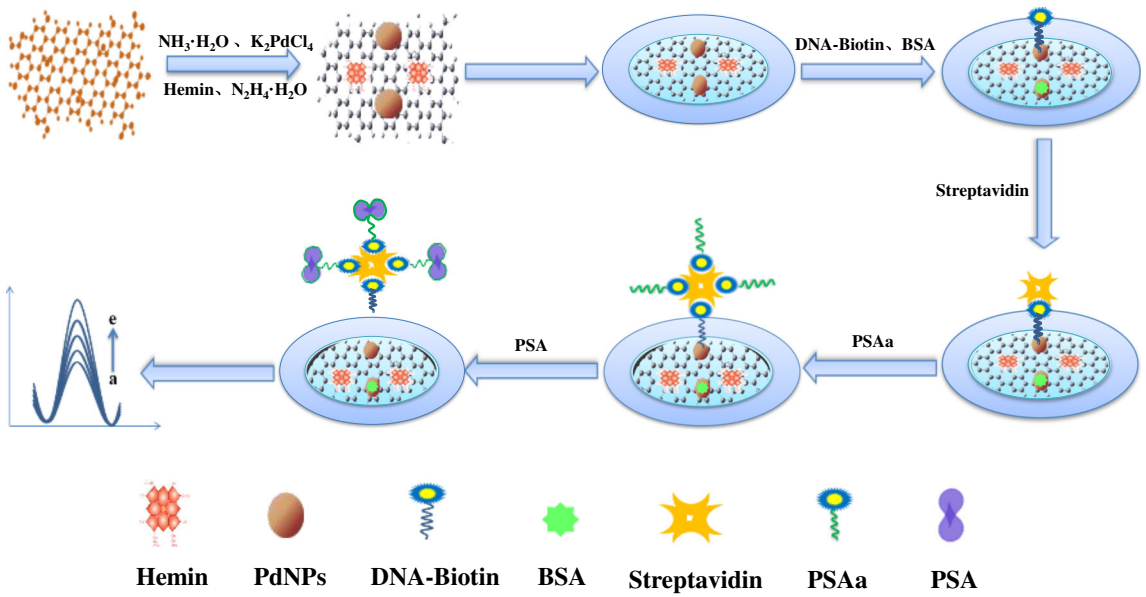

Scheme 1 The procedure for the synthesis of H-Gr/PdNP nanocomposites and the schematic diagrams of the electrochemical aptasensor for PSA detection

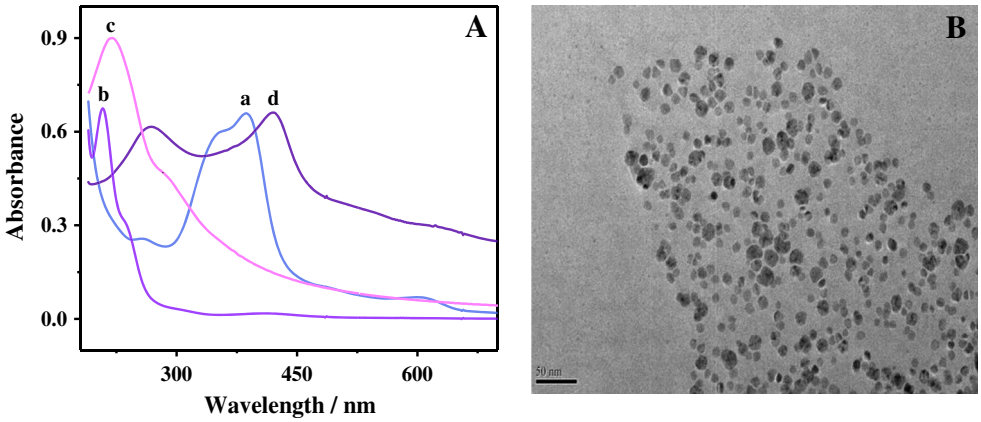

Fig. 1 (A) UV-vis spectra of hemin (a); K_2PdCl_4 solution (b); GO suspension (c) and H-Gr/PdNP suspension (d); (B) The TEM image of H-Gr/PdNP

by the strong affinity of biotin-streptavidin. Thus, the peak current decreases markedly owing to non-conductivity of DNA-Biotin and SA. After PSA is bound to the SA-DNA-Biotin/H-Gr/PdNP/GCE, the electron transfer is impeded. Upon addition of PSA, the PSAa on the electrode surface will recognize the target specifically. Some PSAa-SA-DNA-Biotin has been pulled down from the H-Gr/PdNP due to the weaker interaction of coordination bond. Simultaneously, the signal of hemin increases with the increase of PSA concentration. Thus, a signal amplified electrochemical aptasensor was fabricated successfully for PSA detection.

Choice and characterization of hemin-functionalized graphene conjugated to palladium nanoparticles (H-Gr/PdNPs)

Choice of materials

A large number of nanomaterials have been employed to improve the sensitivity of the analytical method. Graphene has been used as the most common enhanced material for the electrochemical sensors. However, pure graphene makes it easy to aggregate. Hemin can stabilize graphene from aggregating and provide redox probe for electrochemical detection.

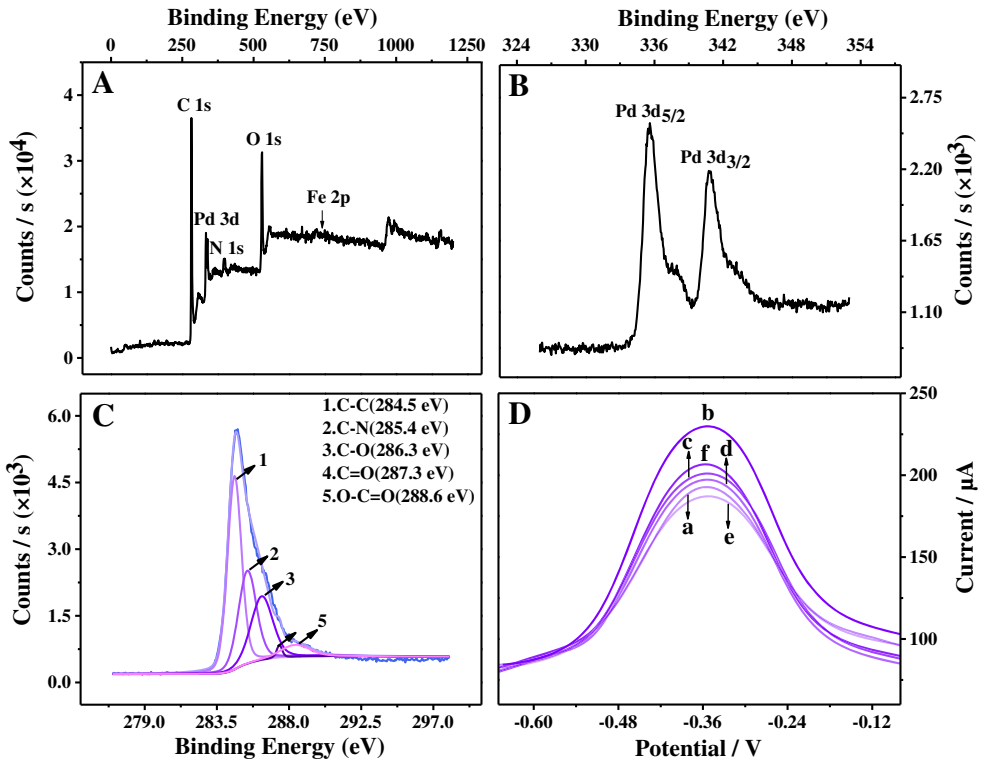

Fig. 2 (**A**) The XPS spectra of H-Gr/PdNP; (**B**) Pd 3d and (**C**) C 1 s; (**D**) DPVs of the H-Gr electrode (curve a); H-Gr/PdNP/GCE (curve b); DNA-Biotin/H-Gr/PdNP/GCE (curve c); SA-DNA-Biotin/H-Gr/PdNP/GCE (curve d); PSAa-SA-DNA-Biotin/H-Gr/PdNP/GCE (curve e); PSAa-SA-DNA-Biotin/H-Gr/PdNP/GCE in 200 ng·mL^{-1} PSA solution (curve f)

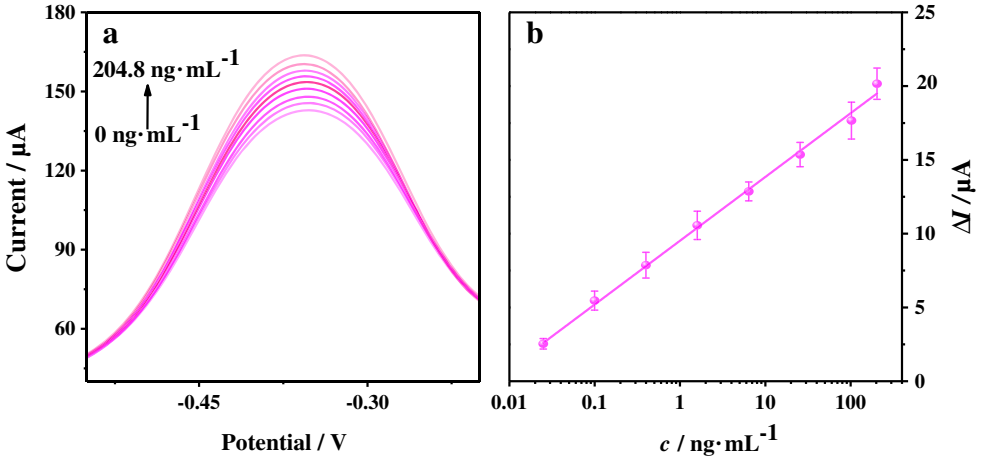

Fig. 3 (**a**) DPVs of the biosensor for different concentrations of PSA: 0, 0.025, 0.10, 0.40, 1.60, 6.40, 25.60, 102.40 and 204.8 ng·mL^{-1} in 6.0 mL 0.10 mol·L^{-1} PBS (pH = 7.4); (**b**) The calibration curve between the peak current changes and the PSA concentration. The measurements were repeated 3 times to obtain the standard deviation. (Amplitude: 50 mV, pulse width: 0.050 s)

Additionally, PdNPs have the advantages of high loading of receptor molecules and unique electro-catalytic property. In the present work, PdNPs can improve the catalytic performance effectively comparing to gold nanoparticles and platinum nanoparticles. They also can provide binding sites for DNA immobilization. Therefore, H-Gr/PdNP is a promising material for the construction of an electrochemical PSA sensor.

Characterization of H-Gr/PdNPs

H-Gr/PdNPs were characterized by UV-vis spectroscopy. As shown in Fig. 1A, hemin (curve a) contains a maximum absorption at 380 nm which is the typical characteristic peak corresponding to the Soret band. A series of weak absorption bands from 500 nm to 700 nm are attributed to the Q-bands of hemin [28]. K_2PdCl_4 solution (curve b) displays a narrow peak at 220 nm. GO dispersion (curve c) exhibits a strong absorption approximately at 230 nm and a shoulder at around 290 nm, which attribute to the π-π* transition of aromatic C-C bonds and the n-π* transition of the C=O bonds, respectively. After forming H-Gr/PdNPs (curve d), the absorption peak of GO shifts from 230 nm to 270 nm and a peak at 441 nm appearing observably, which correspond to the Soret band of hemin with a large bathochromic shift (61 nm). This illustrates that there are π interaction between Gr and hemin. The result confirms the formation of H-Gr/PdNPs. FT-IR spectroscopy also provides some significant information for the successful synthesis of H-Gr (Fig. S1).

TEM shows the morphology of H-Gr/PdNP nanocomposites. As displayed in Fig. 1B, PdNPs are distributed evenly on the surface of H-Gr and the mean size of PdNPs is about 10 nm. This result suggests that PdNPs are successfully attached on the surface of H-Gr. The higher resolution TEM image of H-Gr/PdNP is shown in Fig. S2. The lattice structures of palladium nanoparticles can be observed clearly.

XPS was employed to further characterize the constituent and oxidation states of H-Gr/PdNP nanocomposites. The survey of H-Gr/PdNP shows the presence of C1s, O1s, N1 s, Fe2p and Pd3d (Fig. 2A). $Pd3d_{5/2}$ and $Pd3d_{3/2}$ (Fig. 2B) appears at 335.6 eV and 340.8 eV, respectively [29]. There are five kinds of carbon bonds: C-C (284.5 eV), C-N (285.4 eV), C-O (286.3 eV), C=O (287.3 eV) and O-C=O (288.6 eV) in the C1s spectrum (Fig. 2C). All the above states further imply successful preparation of H-Gr/PdNP.

Stepwise characterization of the aptasensor

To obtain insights on the changes of the stepwise aptasensor, DPV was recorded to characterize the aptasensor. As shown in

Table 1 The comparison of different analytical methods for PSA detection

Platform	Detection Method	Linear Range (ng·mL^{-1})	LOD (pg·mL^{-1})	Reference
Apta–MIP sensor	EIS	0.1-100	1	[12]
SPCE/MoS_2-QD/ PSAAb	EIS	1×10^{-5} - 300	0.01	[30]
G-rich DNA aptamer conjugated 6-FAM	Chemiluminescence	1.9-125	1000	[31]
TH/HRP-pAb	DPV	0.1-100	200	[32]
AuNP / 96-well/SA/MBs	Cleavage of the peptide	0.08-7	30	[33]
H-Gr/PdNP-DNA-Biotin-SA-Aptasensor	DPV	0.025-204.8	8	This work

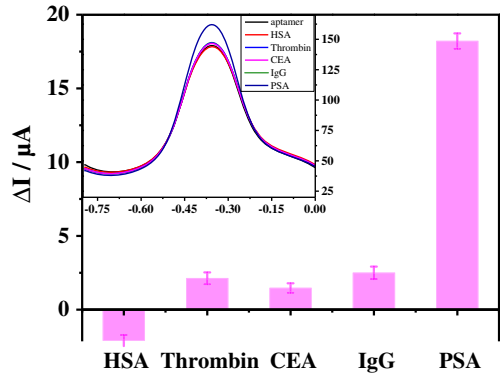

Fig. 4 Selective investigations of the aptasensor for PSA detection. Inset: DPVs of the biosensor respond to the interferents. Error bars show the standard deviations of measurements taken from three times (Amplitude: 50 mV, pulse width: 0.050 s)

Fig. 2D, H-Gr electrode exhibits a distinct oxidation peak at −0.362 V attributing to the oxidation of hemin (curve a) and the peak current dramatically increases after modifying with H-Gr/PdNP (curve b). When DNA-Biotin and SA are modified on the H-Gr/PdNP/GCE successively, the oxidation currents decrease obviously (curve c and d) ascribing to the non-conductivity of the biomolecular. After modifying PSAa on the surface of the SA-DNA-Biotin/H-Gr/PdNP/GCE, the oxidation peak current further decreases (curve e), which attributes the impediment of electron transfer by the biomolecules. However, in the presence of 200 ng·mL^{-1} PSA solution, some PSAa-SA-DNA-Biotin has been pulled away from the electrode. The electron-transfer rates simultaneously increase resulting in the "signal-on" detection of PSA. This illustrates that the PSAa-SA-DNA-Biotin/H-Gr/PdNP/GCE (line f) sensing surface is successfully fabricated.

Optimization of experimental conditions

To obtain the best performance of the sensor, some important optimal experiments were investigated. The following parameters were optimized: (a) the amount of H-Gr/PdNP; (b) the DNA-Biotin concentration; (c) incubation time respective data and figures are given in the Electronic Supporting Material (Fig. S3, Fig. S4, Fig. S5). The following experimental conditions were found to give best results: (a) an amount of H-Gr/PdNP of 8.0 μL; (b) a DNA-Biotin concentration of 5.0 μmol·L^{-1}; (c) an incubation time of 60 min.

Analytical performance of the aptasensor

Under optimized conditions, the electrochemical sensing performance of the PSAa-SA-DNA-Biotin/H-Gr/PdNP/GCE towards PSA was recorded by DPV. The sensing interface was submerged in PBS (pH = 7.4) with different concentrations of PSA varying from 0.025 ng·mL^{-1} to 204.8 ng·mL^{-1}. When PSA was added, PSAa-SA-DNA-Biotin was pulled off from the H-Gr/PdNP due to the specifically combination of PSA and the PSAa and resulting the increase of electron transfer. Thus, the DPV signals increase accordingly (Fig. 3a). As shown in Fig. 3b, the calibration curve shows a good linear relationship between the peak current and the concentrations of PSA. The linear equation express as $\Delta i = 4.3028\ c + 9.5446$ with a correlation coefficient of 0.9981. The detection limit is evaluated to be 8.0 pg·mL^{-1} ($S/N = 3$), which is comparable to the previous works (Table 1). Additionally, the excellent electrochemical-sensing performance may provide a foundation for detecting other biomarkers.

Reproducibility, stability and specificity

The reproducibility of the electrochemical aptasensor was investigated by parallel measurements with the same electrode at least for three times. The identical GCE was pretreated carefully before modification every time, then the same amount of materials and biomolecules were modified to the surface of the electrode. The incubation time was also strictly controlled between the layers. And the peak currents were monitored in 200 ng·mL^{-1} PSA solution. The relative standard deviation (RSD) was 1.7%, illustrating acceptable reproducibility of the sensor. The aptasensor was kept in refrigerator about a month before measurement. 0.58% of the current change was obtained, which ascribed to the excellent stability of the aptasensor.

The specificity of the aptasensor was examined with the interference of thrombin, intravenous gamma globulin (IgG), human serum albumin (HSA) and carcinoembryonic antigen (CEA). 50 times of concentration were added into the electrolyte in succession. The signals were almost unchanged (Fig. 4). When 105 ng·mL^{-1} of PSA was incubated with the aptasensor in the above electrolyte, the peak current increased remarkably indicating satisfied specificity of the PSA aptasensor.

Table 2 The recovery of PSA in human serum samples

Samples	Added (ng·mL^{-1})	Mean Found (ng·mL^{-1} $\bar{x}$ ±s, $n = 3$)	RSD/% (n = 3)	Recovery/%
1	0.06	0.057 ± 0.0006	1.02	95
2	14.4	14.41 ± 0.195	1.35	100.7
3	70	70.23 ± 1.32	1.88	100.3

Application to real sample analysis

In order to evaluate the reliability and feasibility of the electrochemical aptasensor, recovery experiments were performed by standard addition methods [34]. In brief, human serum samples were obtained from local hospital and diluted for 100 times with PBS (pH = 7.4) to reduce the matrix effect of the real sample. Then, different concentrations of PSA were added into the diluted human serums to evaluate the recoveries. The aptasensor was used to detect the target as the methods described above. As can be seen in Table 2, the recoveries of the spiked samples ranges from 95% to 100.3%, which demonstrates the aptasensor can analyze PSA in real clinical samples.

Conclusions

In conclusion, a signal amplified electrochemical aptasensor for PSA determination has been successfully constructed based on H-Gr/PdNP and biotin-streptavidin system. The cooperatively amplified strategy of the hemin-functionalized graphene conjugated to palladium nanoparticles and the biotin-streptavidin system made the sensor more sensitive. The biosensor showed a broad linearity with a relatively low detection limit. It also demonstrated high stability and specificity. Additionally, this strategy has been successfully applied in detection of PSA in human serum, revealing its potential application in clinical diagnosis. Therefore, the electrochemical aptasensor is promising to be an alternative method for PSA detection in real clinical diagnostics. However, at present, the GCE should be pretreated and modified frequently. In future studies, we will overcome this drawback and establish methods to detect different tumor markers simultaneously in clinical diagnosis.

Acknowledgements This research work was supported by the National Natural Science Foundation of China (No. 21775095, 21707082) and the Young "Sanjin" Scholar Foundation of Shanxi Province, 2016

Compliance with ethical standards

The author(s) declare that they have no competing interests.

References

1. Catalona WJ, Smith DS, Ratliff TL, Dodds KM, Coplen DE, Yuan JJJ, Petros JA, Andriole GL (1991) Measurement of Prostate-Specific Antigen in Serum As A Screening-Test for Prostate-Cancer. N Engl J Med 324(17):1156–1161
2. Partin AW, Kattan MW, Subong ENP, Walsh PC, Wojno KJ, Oesterling JE, Scardino PT, Pearson JD (1997) Combination of prostate-specific antigen, clinical stage, and gleason score to predict pathological stage of localized prostate cancer - A multi-institutional update. J Am Med Assoc 277(18):1445–1451
3. Healy DA, Hayes CJ, Leonard P, McKenna L, O'Kennedy R (2007) Biosensor developments: application to prostate-specific antigen detection. Trends Biotechnol 25(3):125–131
4. Oberpenning F, Hetzel S, Weining C, Brandt B, De Angelis G, Heinecke A, Lein M, Fornara P, Schmid HP, Hertle L, Semjonow A (2003) Semi-quantitative immunochromatographic test for prostate specific antigen in whole blood: Tossing the coin to predict prostate cancer? Eur Urol 43(5):478–484
5. Liu S, Zhang X, Wu Y, Tu Y, He L (2008) Prostate-specific antigen detection by using a reusable amperometric immunosensor based on reversible binding and leasing of HRP-anti-PSA from phenylboronic acid modified electrode. Clin Chim Acta 395(1-2): 51–56
6. Liu B, Lu L, Hua E, Jiang S, Xie G (2012) Detection of the human prostate-specific antigen using an aptasensor with gold nanoparticles encapsulated by graphitized mesoporous carbon. Microchim Acta 178(1-2):163–170
7. Zhu Y, Wang H, Wang L, Zhu J, Jiang W (2016) Cascade Signal Amplification Based on Copper Nanoparticle-Reported Rolling Circle Amplification for Ultrasensitive Electrochemical Detection of the Prostate Cancer Biomarker. ACS Appl Mater Interfaces 8(4): 2573–2581
8. Huhtinen P, Soukka T, Lovgren T, Harma H (2004) Immunoassay of total prostate-specific antigen using europium(III) nanoparticle labels and streptavidin-biotin technology. J Immunol Methods 294(1-2):111–122
9. Uludag Y, Tothill IE (2012) Cancer Biomarker Detection in Serum Samples Using Surface Plasmon Resonance and Quartz Crystal Microbalance Sensors with Nanoparticle Signal Amplification. Anal Chem 84(14):5898–5904
10. Chen Y-T, Tuan L-P, Chen H-W, Wei IA, Chou M-Y, Chen H-M, Tyan Y-C, Chen S-F (2015) Quantitative Analysis of Prostate Specific Antigen Isoforms Using Immunoprecipitation and Stable Isotope Labeling Mass Spectrometry. Anal Chem 87(1):545–553
11. Rahi A, Sattarahmady N, Heli H (2016) Label-free electrochemical aptasensing of the human prostate-specific antigen using gold nanospears. Talanta 156–157:218–224
12. Jolly P, Tamboli V, Harniman RL, Estrela P, Allender CJ, Bowen JL (2016) Aptamer–MIP hybrid receptor for highly sensitive electrochemical detection of prostate specific antigen. Biosens Bioelectron 75:188–195
13. Heydari-Bafrooei E, Shamszadeh NS (2017) Electrochemical bioassay development for ultrasensitive aptasensing of prostate specific antigen. Biosens Bioelectron 91:284–292
14. Damborska D, Bertok T, Dosekova E, Holazova A, Lorencova L, Kasak P, Tkac J (2017) Nanomaterial-based biosensors for detection of prostate specific antigen. Microchim Acta 184(9):3049–3067
15. Lin X-Q, Deng H-H, Wu G-W, Peng H-P, Liu A-L, Lin X-H, Xia X-H, Chen W (2015) Platinum nanoparticles/graphene-oxide hybrid with excellent peroxidase-like activity and its application for cysteine detection. Analyst 140(15):5251–5256
16. Zhang L-N, Deng H-H, Lin F-L, Xu X-W, Weng S-H, Liu A-L, Lin X-H, Xia X-H, Chen W (2014) In Situ Growth of Porous Platinum Nanoparticles on Graphene Oxide for Colorimetric Detection of Cancer Cells. Anal Chem 86(5):2711–2718
17. Thanh TD, Balamurugan J, Lee SH, Kim NH, Lee JH (2016) Effective seed-assisted synthesis of gold nanoparticles anchored nitrogen-doped graphene for electrochemical detection of glucose and dopamine. Biosens Bioelectron 81:259–267. https://doi.org/10.1016/j.bios.2016.02.070
18. Singh S, Tuteja SK, Sillu D, Deep A, Suri CR (2016) Gold nanoparticles-reduced graphene oxide based electrochemical immunosensor for the cardiac biomarker myoglobin. Microchim Acta 183(5):1729–1738

19. Lakshmipriya T, Fujimaki M, Gopinath SCB, Awazu K, Horiguchi Y, Nagasaki Y (2013) A high-performance waveguide-mode biosensor for detection of factor IX using PEG-based blocking agents to suppress non-specific binding and improve sensitivity. Analyst 138(10):2863–2870
20. Lakshmipriya T, Gopinath SCB, Tang T-H (2016) Biotin-Streptavidin Competition Mediates Sensitive Detection of Biomolecules in Enzyme Linked Immunosorbent Assay. PLoS One 11(3)
21. Teramura Y, Kuroyama K, Takai M (2016) Influence of molecular weight of PEG chain on interaction between streptavidin and biotin-PEG-conjugated phospholipids studied with QCM-D. Acta Biomater 30:135–143
22. Kong F-Y, Li W-W, Wang J-Y, Fang H-L, Fan D-H, Wang W (2015) Direct electrolytic exfoliation of graphite with hemin and single-walled carbon nanotube: Creating functional hybrid nanomaterial for hydrogen peroxide detection. Anal Chim Acta 884:37–43
23. Tang L, Li S, Xu L, Ma W, Kuang H, Wang L, Xu C (2015) Chirality-based Au@Ag Nanorod Dimers Sensor for Ultrasensitive PSA Detection. ACS Appl Mater Interfaces 7(23): 12708–12712
24. Tzouvadaki I, Jolly P, Lu X, Ingebrandt S, de Micheli G, Estrela P, Carrara S (2016) Label-Free Ultrasensitive Memristive Aptasensor. Nano Lett 16(7):4472–4476
25. Hummers WS, Offeman RE (1958) Preparation of Graphitic Oxide. J Am Chem Soc 80(6):1339–1339
26. Guo Y, Deng L, Li J, Guo S, Wang E, Dong S (2011) Hemin-Graphene Hybrid Nanosheets with Intrinsic Peroxidase-like Activity for Label-free Colorimetric Detection of Single-Nucleotide Polymorphism. ACS Nano 5(2):1282–1290
27. Lv J-J, Wisitruangsakul N, Feng J-J, Luo J, Fang K-M, Wang A-J (2015) Biomolecule-assisted synthesis of porous PtPd alloyed nanoflowers supported on reduced graphene oxide with highly electrocatalytic performance for ethanol oxidation and oxygen reduction. Electrochim Acta 160:100–107
28. Xue S, Yi H, Yuan Y, Jing P, Xu W (2015) A label-free and sensitive electrochemical aptasensor for thrombin based on the direct electron transfer of hemin and hemin@rGO nanosheets as the signal probe. Anal Methods 7(20):8771–8777
29. Zhang Y, Huang Q, Chang G, Zhang Z, Xia T, Shu H, He Y (2015) Controllable synthesis of palladium nanocubes/reduced graphene oxide composites and their enhanced electrocatalytic performance. J Power Sources 280:422–429
30. Kukkar M, Singh S, Kumar N, Tuteja SK, Kim K-H, Deep A (2017) Molybdenum disulfide quantum dot based highly sensitive impedimetric immunoassay for prostate specific antigen. Microchim Acta 184(12):4647–4654
31. Cha T, Cho S, Kim YT, Lee JH (2014) Rapid aptasensor capable of simply diagnosing prostate cancer. Biosens Bioelectron 62:31–37
32. Biniaz Z, Mostafavi A, Shamspur T, Torkzadeh-Mahani M, Mohamadi M (2017) Electrochemical sandwich immunoassay for the prostate specific antigen using a polyclonal antibody conjugated to thionine and horseradish peroxidase. Microchim Acta 184(8): 2731–2738
33. Hun X, Xu Y, Luo X (2015) Peptide-based biosensor for the prostate-specific antigen using magnetic particle-bound invertase and a personal glucose meter for readout. Microchim Acta 182(9-10):1669–1675
34. Cheng Z, Shen Q, Yu H, Han D, Zhong F, Yang Y (2017) Non-enzymatic sensing of hydrogen peroxide using a glassy carbon electrode modified with the layered MoS2-reduced graphene oxide and Prussian Blue. Microchim Acta 184(12):4587–4595